The 8th International Conference on Jets, Wakes and Separated Flows, ICJWSF-2024
September 23-25, 2024, Firenze, Italy

Analysis of the vorticity contributions for a swirling, supersonic aerospike nozzle jet

T. Golliard[1*] and M. Mihaescu[1]

1: Dept. of Engineering Mechanics, FLOW, KTH Royal Institute of Technology, Stockholm, Sweden

[*] Corresponding author: tgol@kth.se

Abstract

Implicit Large Eddy Simulations (ILES) are deployed to characterize the effect of swirling on the terms of the vorticity equation and the aeroacoustic source terms for a cold, supersonic aerospike nozzle jet. Three jets at a Nozzle Pressure Ratio (NPR) = 3 at three different Swirl Numbers $\mathcal{S} = \{0.10, 0.20, 0.30\}$ are simulated. The results are compared with the baseline case without swirl [10]. It is found that swirl leads to a change in vorticity orientation downstream of the aerospike bluff body, thus increasing the contribution of the tilting term to vorticity generation and transport. Furthermore, the supposedly dominating source terms of the inhomogeneous wave equation are counteracted by the interaction of density gradient with the dilatation field. Additional terms linked to the latter as well as entropy noise need to be taken into account to properly represent the source term in all the cases.

Keyword: *Large Eddy Simulations, aerospike nozzle, supersonic jets, aeroacoustics*

1. Introduction

The development of future supersonic aircraft requires overcoming several significant challenges. Among those, addressing jet noise is one of the most demanding. In the past decades, the progress made in numerical simulations and high-performance computing enabled to predict noise emissions for relevant industrial configurations, as well as to come up with sensible noise-reducing techniques. In the context of jets, the conditions at the outlet of the combustion chamber or the turbine dictate the operating regime of the nozzle, and thus affect the flow structures and the resulting aeroacoustic signature of such device. Nozzle operation at non-design conditions leads to increased Sound Pressure Levels (SPL) due to emerging shock cell structures and their interaction with vortical structures. In particular, the effect of swirling boundary condition on the vorticity field and the resulting aeroacoustics has not been addressed for supersonic nozzles. To fill this gap is highly relevant in order to understand the aeroacoustics of Rotating Detonation Combustion (RDC) for instance. In the context of jet noise, the usual numerical approach consists in resolving the relevant source terms and convolute them on a permeable surface using an acoustic analogy. The Lighthill's analogy lays the foundation for such computational techniques [6]. The Lighthill's tensor acting as a source in the inhomogeneous wave equation reads:

$$\mathbf{T} = \rho \mathbf{u}\mathbf{u} + (p - {c_0}^2\rho)\mathbf{I} + \tau, \tag{1}$$

with $\mathbf{u}$ the velocity vector, ρ the density, p the pressure, c_0 the speed of sound in the ambient air, $\mathbf{I}$ the identity matrix and τ the viscous stress tensor. The spatial derivative of the Lighthill's tensor represents the source term of the inhomogeneous wave equation. At low Mach numbers and for isentropic, inviscid flows, it reads:

$$\nabla\nabla : \mathbf{T} = \rho_0 \left[\nabla \cdot (\omega \times \mathbf{u}) + \nabla(\frac{1}{2}u^2) \right], \tag{2}$$

where ω is the vorticity field, $\omega \times \mathbf{u}$ is the Lamb vector and a constant density ρ_0 is assumed. This equation establishes a direct link between vorticity field and sound field. The acoustic analogies developed by Howe and Möhring are based on the previous ansatz [7, 12]. At higher Mach numbers, the vorticity formulation can also provide deeper insight in the flow physics of the jets, if the compressibility effects are taken into account. Moreover, previous investigations have highlighted the role of coherent structures in sound generation mechanisms [8]. In that regard, vorticity characterization is essential to gain deeper understanding of the physical mechanisms at play behind sound generation. In supersonic configurations, the interaction of vortices with shocks is a fundamental sound source. Previous studies on the effect of swirl for the aerospike nozzle jet showed that shock-cell structures downstream of the aerospike body could be suppressed, reducing the effect of shock-associated noise [11]. However, the present analysis allows to characterize vorticity transport and coherent structures without distinguishing between shock-free regions and regions featuring shocks. The complete aeroacoustic analysis regarding jet modes, screech and global SPL after applying the Ffowcs Williams-Hawkings equation is found in [11]. In the present paper, the computational approach is presented in Section 2 and the results are discussed in Section 3.

2. Computational approach

Implicit Large Eddy Simulations (ILES) of an annular supersonic, swirling, cold jet exhausting an axisymmetric aerospike nozzle are performed. A previous study focusing more specifically on the flow characteristics and the resulting aeroacoustic signature for this jet was conducted. The computational approach was described in detail there; a short overview is given in the present paper. The interested reader may refer to [10, 11]. The simulations are performed using an in-house finite volume-based compressible flow solver. A second order central difference scheme in space and an explicit four-stage Runge-Kutta scheme for the time integration are used. A modified artificial dissipation after Jameson is used to capture shock waves and avoid Gibbs-like oscillations near shocks. Further details about the tuning of the dissipation coefficients can be found in [9]. The computational approach used in this paper has been validated for various nozzle geometries and boundary conditions by comparing near- and far-field acoustic measurements as well as PIV measurements with the flow characteristics provided by the solver [4, 9].

The geometry consists of a three-dimensional, axisymmetric aerospike nozzle embedded in a straight annular duct. The annular duct has an equivalent diameter of $D_{eq} = 84.7$ mm, which is the diameter the nozzle would have if it were circular. All geometric parameters are made dimensionless using this equivalent diameter. The axisymmetric, three-dimensional aerospike body is $2.08D_{eq}$ long. The structured grid consists of 119 blocks making up for 170 million cells. It is $65D_{eq}$ long in total and has a diameter of $44D_{eq}$ at the far-field outlet boundary downstream.

A total pressure of $304,000$ Pa and total temperature of 293 K are applied at the nozzle inlet. The Swirl Number is defined as follows:

$$\mathcal{S} = \frac{\int \rho r u_\theta u_z dA}{D_{eq} \int \rho u_z u_z dA} \tag{3}$$

where u_θ is the azimuthal velocity, u_z is the axial velocity and dA is a surface element normal to the flow direction. Three Swirl Numbers $\mathcal{S} = 0.10, 0.20, 0.30$ are applied at the inlet of the annular nozzle by prescribing the velocity vector. Characteristic boundary conditions are applied at the far-field boundaries with a static pressure $p = 101,325$ Pa. Additionally, a mesh stretching strategy is used to dissipate acoustic waves generated in the potential core. Adiabatic no-slip boundary conditions are applied in the annular chamber and at the aerospike body in a weak sense. Further details about the computational strategy and the mesh size can be found in [11].

3. Vorticity contributions of a supersonic, cold aerospike nozzle jet

3.1. Motivation

Equation 2 shows a direct link between vorticity fields and sound generation. In the supersonic regime, vortical structures interacting with shocks are stretched and become a powerful sound source, as was shown by Ribner [3], making the treatment of vorticity and sound generation even more complex. The various contributions from the vorticity equation are analyzed in this paper to shed new light on the vorticity generation and transport in a swirling, supersonic nozzle jet. The vorticity equation reads:

$$\frac{\partial \omega}{\partial t} + (\mathbf{u} \cdot \nabla)\omega = (\omega \cdot \nabla)\mathbf{u} - \omega(\nabla \cdot u) + \frac{1}{\rho^2}\nabla\rho \times \nabla p, \tag{4}$$

where the effect of viscosity is neglected. The left-hand side consists of the time derivative of the vorticity and the convection term. The two first terms on the right-hand side feature the stretching and tilting terms due to velocity gradients and compressibility. The last term represents baroclinicity emerging due to the non-alignment of density and pressure gradients. In particular, the latter term gains in importance in highly-heated jets. Projecting the contribution of the velocity gradient and compressibility terms along one flow direction, for instance in x-direction, yields:

$$[(\omega \cdot \nabla)\mathbf{u} - \omega(\nabla \cdot u)]_x = \omega_y \frac{\partial u_x}{\partial y} + \omega_z \frac{\partial u_x}{\partial z} - \omega_x \left(\frac{\partial u_y}{\partial y} + \frac{\partial u_z}{\partial z} \right). \tag{5}$$

The two first terms on the right-hand side correspond to the orientation change of vorticity, the so-called tilting term. Tilting enhances vortex reconnection. Investigations of subsonic jets showed that vortex reconnection is a significant sound source and that its effect on the SPL is scaling with the jet Mach number [2]. The second term featuring ω_x as a pre-factor corresponds to the stretching associated with the area change of a vortex.

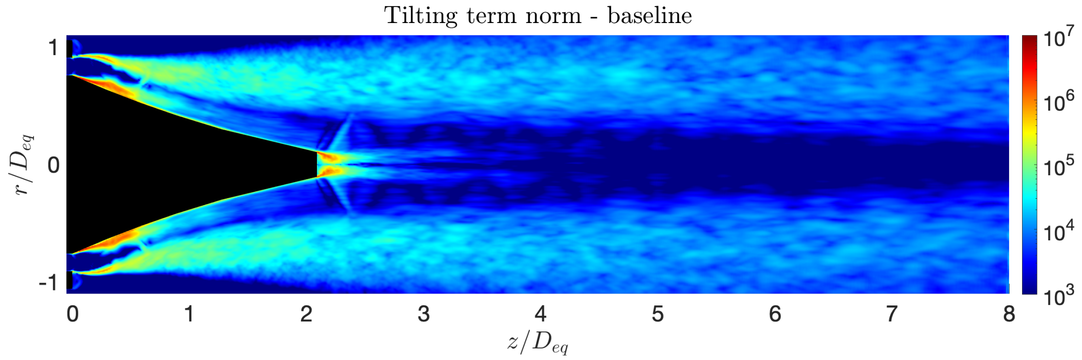

(a) Baseline case.

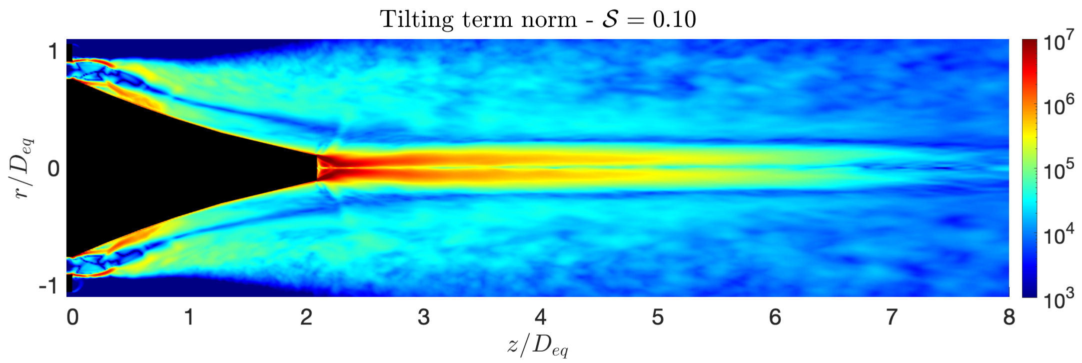

(b) Case $\mathcal{S} = 0.10$.

Fig. 1: Time-averaged tilting term (Eq. 5).

Figure 1 shows that the tilting term is enhanced at the location of the shear layer when applying swirling boundary conditions at the nozzle inlet. This increase is attributable to the additional shear component in azimuthal direction. The term magnitude reaches its maximum downstream of the aerospike bluff body around $z/D_{eq} \sim 2.2$. For brevity's sake, only the two-dimensional profiles for the baseline case and Swirl Number $\mathcal{S} = 0.10$ are presented. The contributions of the different terms integrated over a cross-section will be shown for the remaining cases in Sections 3.2 and 3.3.

3.2. Integrated vorticity contributions

Figure 2 displays the norm of the stretching and tilting terms defined in Eq. 5 as a function of the distance in the streamwise direction z integrated over a cross-section normal to the streamwise direction. The tip of the aerospike nozzle is marked by a dashed line at $z/D_{eq} = 2.08$ separating two flow regions: one in the vicinity of the aerospike bluff body called the annular region, and another downstream of it called the circular region. The effect of compressibility is dominant in the annular region where a shock-cell structure is formed in all the cases. Swirling boundary conditions lead to a flow acceleration towards the tip of the aerospike nozzle around $z/D_{eq} \sim 1.5$, and an enhanced contribution of the stretching term on vorticity generation.

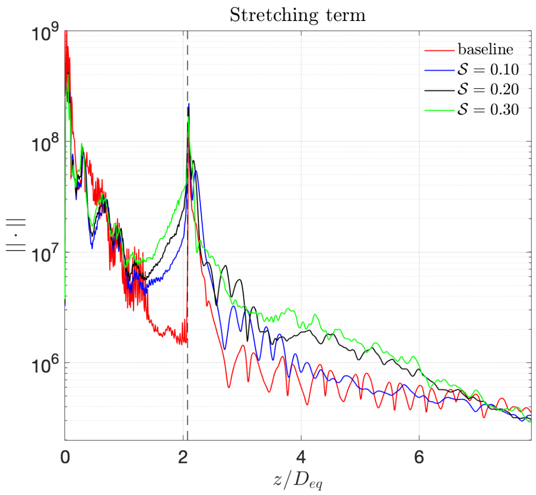

(a) Baseline case.

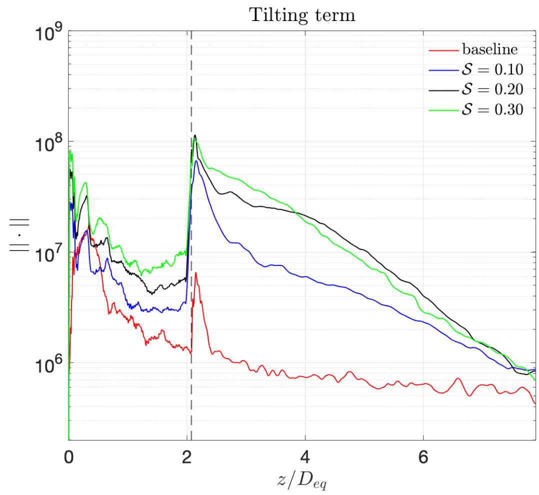

(b) Case $\mathcal{S} = 0.10$.

Fig. 2: Norm of the stretching and tilting term integrated over a cross-section as a function of z/D_{eq}.

The stretching contribution is highest for the case $\mathcal{S} = 0.30$ downstream of the aerospike body but within the same range as for the baseline case. The latter case features similar orders of magnitude for tilting and stretching terms in the circular region. For increasing Swirl Numbers, the tilting term becomes dominant. It is due to the change of vorticity orientation illustrated in Fig. 1b, linked to the formation of an inner annular shear layer at radial distance $r/D_{eq} \sim 0.10$. This change in vorticity orientation is correlated to vortex reconnection which was shown to be a significant sound source in the subsonic range [2].

3.3. Inhomogeneous wave equation and theory of vortex sound

Let us now analyze the contribution of the various source terms of the inhomogeneous wave equation. One can rewrite the source term as follows:

$$\nabla\nabla : \mathbf{T} = \nabla \cdot [\rho(\omega \times \mathbf{u})] + \nabla \cdot \left[\rho \frac{\nabla |u|^2}{2}\right] + \nabla \cdot [(\nabla \cdot (\rho \mathbf{u}))\mathbf{u}] + \left(\nabla^2 p - {c_0}^2 \nabla^2 \rho\right), \tag{6}$$

where the viscous effects have been neglected. The first term on the right-hand side is the divergence of the Lamb vector. It can be explicitly written as follows:

$$\nabla \cdot [\rho(\omega \times \mathbf{u})] = (\rho \mathbf{u}) \cdot (\nabla \times \omega) + \mathbf{u} \cdot (\nabla p \times \omega) - \rho(\omega \cdot \omega). \tag{7}$$

The first term in Eq. 7 corresponds to the flexion product and characterizes the conversion of angular momentum of a vortex into linear momentum. The last term corresponds to the negative enstrophy. These two terms are the main sound sources in inviscid, incompressible and isentropic jets. The second term in Eq. 7 is an important contribution in mixing layers. The second term on the right-hand side of Eq. 6 corresponds to the spatial variation of kinetic energy and can be decomposed as follows:

$$\nabla \cdot \left[\rho \frac{\nabla |u|^2}{2}\right] = \rho \nabla^2 \left(\frac{|u|^2}{2}\right) + \nabla \rho \cdot \nabla \frac{|u|^2}{2}. \tag{8}$$

In supersonic cases, the deviation from the isentropic condition depicted by the last term in Eq. 6 is an important source term. The last part of the paper will show that this term cannot be neglected if one wants to properly compute the source term. Previous investigations emphasized the effect of the flexion product and the enstrophy (see Eq. 7), as well as the Laplacian of the kinetic energy for sound generation (Eq. 8)[1, 5]. In the following, these three terms will be referred to as the dominant terms.

Figure 3 shows the magnitude of the source term given in Eq. 6, the dominant terms and the sum of the two first terms explicitly written in Eq. 7 and 8, called $1 + 2$, for the baseline case and Swirl Numbers $\mathcal{S} = \{0.10, 0.20\}$. Those terms are integrated over a cross-section normal to the streamwise direction. The

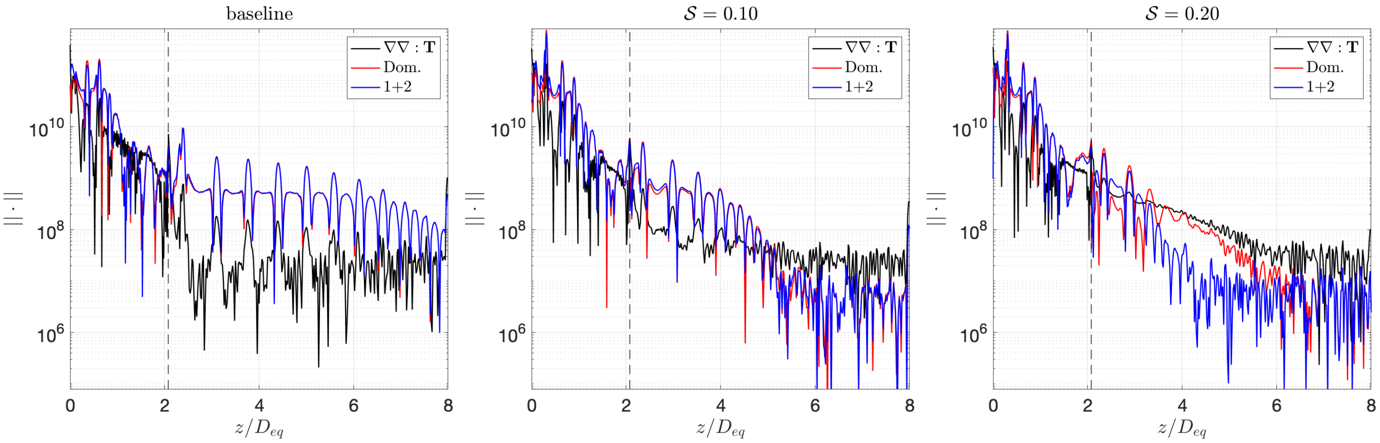

(a) Baseline case. (b) Case $\mathcal{S} = 0.10$. (c) Case $\mathcal{S} = 0.20$.

Fig. 3: Magnitude of the complete source $\nabla\nabla : \mathbf{T}$, the dominant terms and the two first terms on the right hand side of Eq. 6.

results for $\mathcal{S} = 0.30$ are very similar to those of $\mathcal{S} = 0.20$ and are not shown here for brevity's sake. The regions featuring shocks display the same order of magnitudes for the dominant terms and the two first terms (around 5×10^9). However, the global source term's magnitude is lower in the circular region (around 10^7), which indicates that other sound generation mechanisms counteract the dominant terms. On the other hand, the dominant term features the same order of magnitude around 10^8 as the general source term on Fig. 3c in the range $z/D_{eq} = 3 - 6$ for $\mathcal{S} = 0.20$. Nevertheless, these terms do not overlap with the sum of terms $1 + 2$. This suggests that despite the order of magnitude being correct, the dominant terms are damped by the left out terms in Eq. 7 and 8, meaning that those cannot longer be neglected.

The interaction between the dilatation and the density gradients corresponds to the third term on the right hand-side in Eq. 6. It reads:

$$\nabla \cdot [(\nabla \cdot (\rho \mathbf{u}))\mathbf{u}] = \rho [\nabla(\nabla \cdot \mathbf{u})] \cdot \mathbf{u} + (\nabla \cdot \mathbf{u})^2 \rho + 2(\nabla \cdot \mathbf{u})\nabla\rho \cdot \mathbf{u} + \mathbf{u} \cdot (\mathbf{u} \cdot \nabla\nabla\rho) + \mathbf{u} \cdot (\nabla \mathbf{u} \nabla \rho) \quad (9)$$

An analysis of the terms of Eq. 9 shows that the first and fourth terms are dominant. Furthermore, the deviation from the isentropic condition found in Eq. 6 exhibits a comparable order of magnitude as these two terms in the circular region for all the cases (around 10^8). For brevity's sake, a detailed analysis of each contribution is not presented here. However, we propose to rewrite the source term by taking into account the aforementioned additional contributions. The modified source terms S_1 and S_2 read:

$$\begin{aligned} S_1 &= (\rho \mathbf{u}) \cdot (\nabla \times \omega) - \rho(\omega \cdot \omega) + \rho \nabla^2 \left(\frac{|u|^2}{2} \right) + \rho [\nabla(\nabla \cdot \mathbf{u})] \cdot \mathbf{u} + \mathbf{u} \cdot (\mathbf{u} \cdot \nabla\nabla\rho) + \left(\nabla^2 p - {c_0}^2 \nabla^2 \rho\right) \\ S_2 &= \nabla \cdot [\rho(\omega \times \mathbf{u})] + \nabla \cdot \left[\rho \frac{\nabla |u|^2}{2} \right] + \rho [\nabla(\nabla \cdot \mathbf{u})] \cdot \mathbf{u} + \mathbf{u} \cdot (\mathbf{u} \cdot \nabla\nabla\rho) + \left(\nabla^2 p - {c_0}^2 \nabla^2 \rho\right) \end{aligned} \quad (10)$$

The norm of the proposed source terms integrated over a cross-section normal to the streamwise direction are compared with the norm of the Lighthill's tensor derivative and the dominant terms on Fig. 4. S_1 slightly overpredicts the general source term, whereas S_2 is matching it satisfyingly, even in flow regions featuring shocks. This suggests that the remaining non-dominant terms in Eq. 8 and 7 need to be taken into account. Furthermore, the incorporation of the dominant terms due to compressibility effects found in Eq. 9 as well as the deviation from the isentropic case allow to reach the correct order of magnitude, in particular downstream of the aerospike bluff body for $\mathcal{S} = 0.20$.

4. Conclusion

Large Eddy Simulations of a cold, swirling aerospike nozzle jet were performed to analyze the vorticity field and the associated aeroacoustic sources. It was found that the tilting term linked with the change of

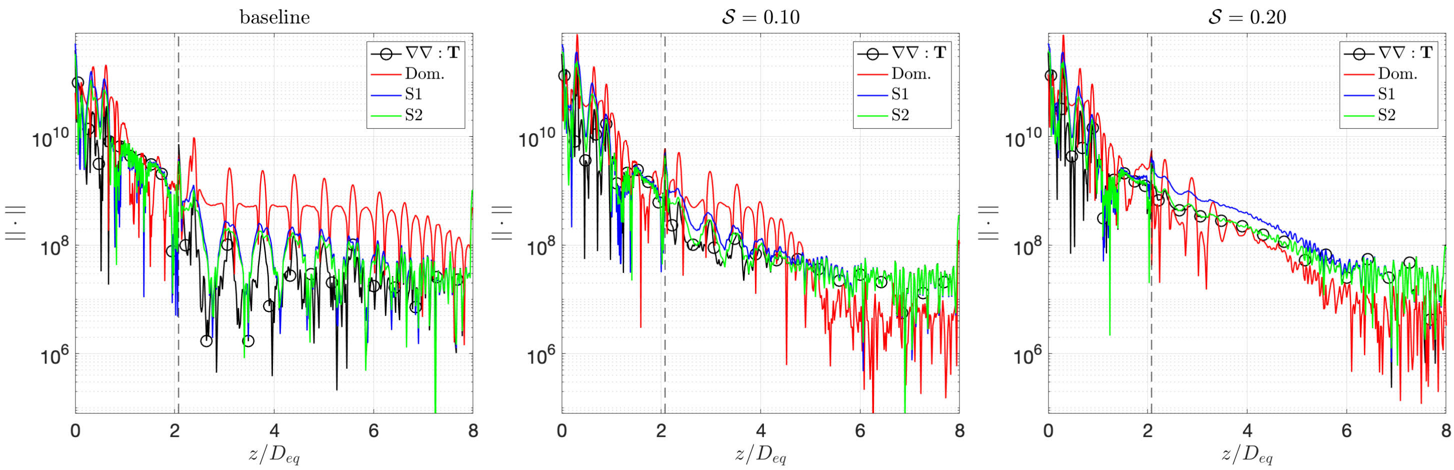

(a) Baseline case. (b) Case $\mathcal{S} = 0.10$. (c) Case $\mathcal{S} = 0.20$.

Fig. 4: Norm of the complete source term, the dominant terms and the source terms given in Eq. 10.

vortex orientation was enhanced. Furthermore, we showed that interactions between density gradient and dilatation field as well as the deviation from the isentropic condition need to be taken into account to properly represent the source term of the inhomogeneous wave equation.

Acknowledgments

This project is funded by the ”INSPIRE” EU Project H2020- MSCA-ITN-2020, Marie Skłodowska-Curie Innovative Training Networks, Project No. 956803. The computations were performed on resources provided by the National Academic Infrastructure for Supercomputing in Sweden (NAISS) at the PDC Centre for High-Performance Computing (PDC-HPC) and at the National Supercomputer Center (NSC) in Sweden.

References

[1] Golanski F., Fortuné V., and Lamballais E. “Noise radiated by a non-isothermal, temporal mixing layer”. In: *Theoretical and Computational Fluid Dynamics* 19.6 (2005).

[2] Daryan H., Hussain F., and Hickey J-P. “Sound generation mechanism of compressible vortex reconnection”. In: *Journal of Fluid Mechanics* 933.A34 (2022).

[3] Ribner H. “Convection of a pattern of vorticity through a shock wave”. In: *NASA Report* (1954).

[4] Ahn M-H. et al. “Large-eddy simulations of flow and aeroacoustics of twin square jets including turbulence tripping”. In: *Physics of Fluids* 35.6 (2023).

[5] Cabana M., Fortuné V., and Jordan P. “Identifying the radiating core of Lighthill’s source term”. In: *Theor. Comput. Fluid Dyn.* 22 (2008).

[6] Lighthill M.J. “On sound generated aerodynamically I. General theory”. In: *Proceedings of the Royal Society A* 211.1107 (1952).

[7] Howe M.S. “Chapter 5: Vortex Sound”. In: *Theory of Vortex Sound*. 2003.

[8] Jordan P. and Colonius T. “Wave Packets and Turbulent Jet Noise”. In: *Ann. Review of Fluid Mechanics* 45.1 (2013).

[9] Gojon R. et al. “Temperature effects on the aerodynamic and acoustic fields of a rectangular supersonic jet”. In: *AIAA Paper* (2017).

[10] Golliard T. and Mihaescu M. “Computational aeroacoustics for a cold, non-ideally expanded aerospike nozzle”. In: *Journal of Turbomachinery* 146.2 (2024).

[11] Golliard T. and Mihaescu M. “Swirling flow effects on the aeroacoustic signature of an aerospike nozzle”. In: *ASME Proceedings* (2024).

[12] Möhring W. “On vortex sound at low Mach number”. In: *Journal of Fluid Mechanics* 85.4 (1978).